REMARKS

Favorable reconsideration is respectfully requested in view of the foregoing amendments and the following remarks.

Applicants sincerely thank the Examiner for holding an interview with Applicants' representative. The Examiner's kind suggestions have been incorporated into this response.

I. CLAIM STATUS AND AMENDMENTS

Claims 9-12, 17 and 18 were pending in this application when last examined and stand rejected.

Claims 9 and 18 are amended. Support for the amendment to claim 9 can be found on page 6, lines 22-23, of the specification as filed. Claim 18 is amended to clarify the claimed invention.

No new matter has been added.

II. UTILITY REJECTION

On pages 2 and 3 of the Office Action, claims 9-12 and 17-18 were rejected under 35 U.S.C. § 101 as directed to non-statutory subject matter. The claims have been amended to recite "isolated" as recommended by the Examiner and therefore this rejection is overcome.

III. WRITTEN DESCRIPTION

In item 5 on pages 3-5 of the Office Action, claims 9-12 and 17-18 were rejected under 35 U.S.C. § 112, first paragraph, as failing to meet the written description requirement.

Applicants respectfully traverse this rejection as applied to the amended claims.

As recommended by the Examiner during the interview, claim 9 is amended to indicate that the polynucleotide encoding a chimeric protein composed of *Vargula* luciferase and YFP comprises the sequence of SEQ ID NO: 1. Thus, claim 9 now recites a concrete structure for a species of claim 9.

Furthermore, attached herein are the following two references:

Reference A – Proc Natl Acad Sci USA Vol.86, pp6567-6571(1989); and

Reference B – Proc Natl Acad Sci USA Vol.94, pp3402-3407(1997).

Reference A describes: "The marine ostracod crustacean *Vargula hilgendorfii*, formally *Cypridina hilgendorfii* ..." (p. 6567, left column, lines 21-22). Reference B describes "the ostracod *Cypridina* (or *Vargula*)" (p.3403, right column, second paragraph, line 2). In view of these references, it is apparent that *Cypridina* luciferase and *Vargula* luciferase are so closely related that possession of *Vargula* luciferase/YFP chimeric indicates that the inventors had possession of *Cypridina* luciferase/YFP chimeric. Thus, Applicants note that, as applied to the amended claims, this rejection is overcome.

CONCLUSION

In view of the foregoing amendments and remarks, it is respectfully submitted that the present application is in condition for allowance and early notice to that effect is hereby requested.

If the Examiner has any comments or proposals for expediting prosecution, please contact the undersigned attorney at the telephone number below.

Respectfully submitted,

Yoshihiro OHMIYA et al.

By: [signature]
William R. Schmidt, II
Registration No. 58,327
Attorney for Applicants

WRS/lc
Washington, D.C. 20006-1021
Telephone (202) 721-8200
Facsimile (202) 721-8250
August 18, 2008

Proc. Natl. Acad. Sci. USA
Vol. 86, pp. 6567–6571, September 1989
Biochemistry

Cloning and expression of cDNA for the luciferase from the marine ostracod *Vargula hilgendorfii*

(bioluminescence/oxygenase/luciferin/aequorin/gene expression)

ERIC M. THOMPSON*, SHIGEKAZU NAGATA*, AND FREDERICK I. TSUJI*†

*Osaka Bioscience Institute, 6-2-4 Furuedai, Suita, Osaka 565, Japan; and †Marine Biology Research Division, Scripps Institution of Oceanography, University of California at San Diego, La Jolla, CA 92093

Communicated by Martin D. Kamen, June 7, 1989 (received for review May 12, 1989)

ABSTRACT **The marine ostracod *Vargula hilgendorfii* ejects luciferin and luciferase into seawater to produce a bright luminous cloud. The light is due to the oxidation of luciferin, an imidazopyrazine compound, by molecular oxygen, catalyzed by luciferase. The mechanism of the reaction has been studied extensively and the 60 kcal/mol required for the blue emission have been shown to be derived from the oxidation of luciferin via a dioxetanone intermediate, in which the excited state oxyluciferin bound to luciferase is the emitter. However, only limited information is available regarding the properties of the enzyme. This paper reports the cloning and sequence analysis of the cDNA for *Vargula* luciferase and the expression of the cDNA in a mammalian cell system. The primary structure, deduced from the nucleotide sequence, consists of 555 amino acid residues in a single polypeptide chain with a molecular weight of 62,171. Two regions of the enzyme show significant amino acid sequence homology with an N-terminal segment of the photoprotein aequorin. The *Vargula* luciferase gene, which contains a signal sequence for secretion, should be well suited as a reporter in studies of gene expression.**

The marine ostracod crustacean *Vargula hilgendorfii* (1), formerly *Cypridina hilgendorfii* (2), has played a central role in contributing to an understanding of the chemical and physical bases of bioluminescence. *V. hilgendorfii* is indigenous to the south coastal waters of Japan, where it is commonly referred to as "umi botaru" or the "sea firefly." In the past the animal occurred in great abundance, but their numbers have been reduced significantly in recent years. The earliest studies on the bioluminescence of *V. hilgendorfii* were carried out by Harvey (3), and subsequent studies by various investigators resulted in numerous publications (4).

V. hilgendorfii is a small animal (≈3 mm long) with nocturnal habits. It lives in sand at the bottom of shallow waters and becomes an active feeder at night. When disturbed it ejects a copious secretion of luciferin (substrate) and luciferase into sea water, producing a bright luminous cloud. The light results from an enzyme–substrate reaction, catalyzed by luciferase, in which luciferin, an imidazopyrazine compound, is oxidized by molecular oxygen (1, 5). The other products of the reaction are oxyluciferin and carbon dioxide (6, 7). The excited-state oxyluciferin bound to luciferase is the emitter in the reaction (8). Following the determination of the imidazopyrazine structure of *Vargula* luciferin (5), it was found that imidazopyrazine compounds are widely used as substrates in the bioluminescence reactions of marine organisms. One such reaction which has been studied in detail is that of the jellyfish *Aequorea victoria*, from which the cDNA for the calcium-binding photoprotein aequorin has recently been cloned (9, 10).

Interestingly, *V. hilgendorfii* luciferin, or a compound almost identical to it, is used as a substrate by luminescent fish. These include the North American batrachoidid fish *Porichthys notatus*, which possesses more than 700 dermal light organs (11); apogonid fishes of the Far East, in which the light organs are connected to the digestive tract by a duct (12); and the Japanese pempherid fish *Parapriacanthus ransonneti*, in which the light organ communicates directly with the pyloric caeca (13). The luciferins and luciferases of all of these animals give reciprocal light-emitting cross-reactions with *Vargula* luciferin and luciferase. Since luminescent *Vargula* is found in the same waters as these fishes, questions have been raised as to the origin of their luciferins and luciferases (14).

The present study reports the cloning and nucleotide sequence analysis of the cDNA for *Vargula* luciferase and the expression of this cDNA in a mammalian cell system.‡ Because of the use of imidazopyrazine compounds by taxonomically diverse marine organisms and since the primary structure of aequorin is the only one presently known, it is of interest to compare the structures of *Vargula* luciferase and aequorin. The study of the structures of these two proteins and others should lead to a better understanding of how bioluminescent reactions take place and how the luminescent systems of various marine organisms are related evolutionarily.

MATERIALS AND METHODS

Purification and Sequencing of *Vargula* Luciferase. *Vargula* luciferase, partially purified as described (15), was purified to homogeneity, first by using a tryptamine affinity column (Pierce) equilibrated in 2.0 M NaCl/0.07 M Tris·HCl, pH 7.2, and eluting stepwise with 30% (vol/vol) ethylene glycol/0.17 M NaCl/0.07 M Tris·HCl, pH 7.2, and second, after concentration by ultrafiltration, by using a *p*-aminobenzamidine affinity column (Pierce) under the same chromatographic conditions (F.I.T., unpublished work). Aliquots (120 μg) of the purified protein were subjected to endopeptidase digestions by trypsin (Boehringer Mannheim), lysyl endopeptidase (Wako Pure Chemical, Osaka, Japan) or arginyl endopeptidase (Takara Shuzo, Kyoto, Japan). Peptide fragments were separated by reverse-phase chromatography on a C_{18}-protein-peptide HPLC column (Vydac). Undigested luciferase and purified peptides were sequenced by Edman degradation using a gas-phase protein sequenator (Applied Biosystems; model 477A).

mRNA Preparation and cDNA Library Construction. *V. hilgendorfii* were collected (15) at Chiba, Japan, and frozen immediately in liquid nitrogen. The ostracods (wet weight, 5 g) were ground to a fine powder in liquid nitrogen with an ultraturrax homogenizer (Janke & Kunkel, Staufen, F.R.G.). Total cellular RNA was extracted from the powder by the

The publication costs of this article were defrayed in part by page charge payment. This article must therefore be hereby marked "*advertisement*" in accordance with 18 U.S.C. §1734 solely to indicate this fact.

‡The sequence reported in this paper has been deposited in the GenBank data base (accession no. M25666).

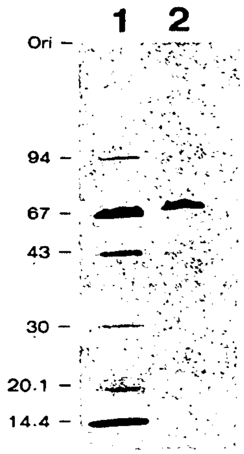

FIG. 1. NaDodSO$_4$/polyacrylamide gradient gel electrophoresis of purified *Vargula* luciferase. Samples were analyzed on a 10–15% PhastGel (Pharmacia) gradient and proteins were visualized by using a PhastGel silver staining kit (Pharmacia). Lane 1, Pharmacia low molecular weight markers (M_r given × 10^{-3}); lane 2, 50 ng of affinity chromatography purified *Vargula* luciferase.

guanidine thiocyanate/cesium chloride method (16) and poly(A)$^+$ RNA was purified by oligo(dT)-cellulose column chromatography (17). The cDNA library was constructed as described (18) except that the double-stranded *Eco*RI digested cDNA was size-selected by two purifications on low-melting agarose (Bio-Rad).

Screening and Analysis of cDNA Clones. Peptide sequences with minimum codon ambiguity were used to synthesize oligonucleotide probes by the phosphoramidite method (19), using a DNA synthesizer (Applied Biosystems; Model 381A). The oligonucleotide probes were 5′-end-labeled (specific activity, 5–6 × 10^6 cpm/pmol) with T4 polynucleotide kinase (Takara Shuzo) and [γ-^{32}P]ATP (222 TBq/mmol; New England Nuclear) and used to screen 1 × 10^6 recombinant phages by plaque hybridization (20). Hybridization conditions were as described (21) except that the hybridization temperature was lowered to 28°C and the filters were washed at 37°C with 1× SSC (0.15 M NaCl/15 mM sodium citrate, pH 7.0). *Eco*RI fragments of positive clones were subcloned in pUC8 and nucleotide sequence analyses were carried out by the dideoxynucleotide chain termination technique (22, 23) using a 7-deaza sequencing kit (Takara Shuzo) and [α-^{32}P]dCTP (222 TBq/mmol) (New England Nuclear).

Expression of *Vargula* Luciferase. *Hin*dIII and *Bgl* II linkers (Takara Shuzo) were ligated to *Vargula* luciferase cDNA at the 5′ and 3′ ends, respectively. The plasmid pRSVL (obtained from S. Subramani, Univ. of California, San Diego) (24) was digested with *Sma* I and ligated with *Bgl* II linker. The linearized plasmid and the cDNA were digested with *Hin*dIII and *Bgl* II and the *Hin*dIII–*Bgl* II fragment containing *Vargula* luciferase cDNA was inserted in place of the firefly luciferase cDNA. The expression vector was designated pRSVVL.

Monkey COS cells (25) (7 × 10^6) were seeded on 10-cm dishes in 10 ml of Dulbecco's modified Eagle's medium (Nissui Seiyaku, Tokyo) containing 10% fetal calf serum (HyClone). The cells were transfected with 10 μg of plasmid DNA containing the cDNA insert by using the calcium phosphate method (26, 27). After 48 hr of incubation, the medium was collected and the cells were harvested. Cell extracts were prepared by repeated cycles of freezing and thawing followed by centrifugation (24). To assay for *Vargula* luciferase activity, aliquots of the medium and of the cell extract were diluted with 200 mM Tris·HCl, pH 7.6 (total volume of 1.5 ml) in a 20-ml scintillation vial and placed in a Mitchell–Hastings photometer (28). *Vargula* luciferin, prepared as described (15), was dissolved at 50 nM in 200 mM sodium phosphate buffer, pH 6.8, and 1.5 ml of this solution was injected into the scintillation vial. Conversion of light intensity to quanta per second was made by calibrating the photometer with a [^{14}C]-hexadecane light standard (29).

RESULTS

Peptide Sequences and Probe Design. When analyzed by polyacrylamide gel electrophoresis in the presence of NaDodSO$_4$, the purified *Vargula* luciferase showed a single band of M_r 68,000 (Fig. 1). Edman degradation of the intact protein did not yield an assignable amino acid, suggesting that the N terminus is blocked. The luciferase was then digested with endopeptidases, and several peptides were subjected to Edman degradation.

A portion of one of the peptide fragments had the sequence Thr-Met-Glu-Asn-Leu-Asp-Gly-Gln-Lys, which was used to design the complementary oligodeoxynucleotide probe 5′-(T/C)TT(T/C)TGICC(A/G)TCIAGGTT(T/C)TCCATIGT-3′. Deoxyinosine (30) was included at three positions where there was high codon degeneracy. A second complementary probe with A substituted for G at position 15 was also synthesized, and a mixture of these two probes was used to screen the *Vargula* cDNA library. Using the plaque hybridization technique (20), we isolated eight positive clones from the library; two of these, designated VL16 and VL18, with insert lengths of 1.2 and 1.5 kilobases (kb), were selected for further analysis.

Nucleotide Sequence of *Vargula* Luciferase. The restriction map of *Vargula* luciferase cDNA was constructed by using clones VL16 and VL18 as shown in Fig. 2. Clones VL16 and VL18 each had a single internal *Eco*RI site and had a

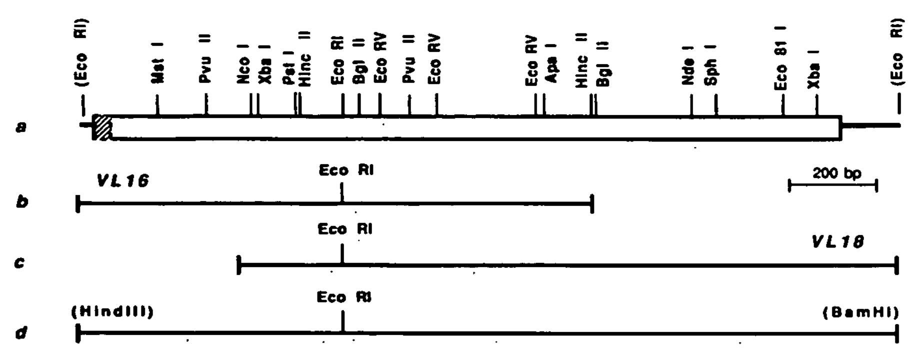

FIG. 2. Restriction map of *Vargula* luciferase cDNA and strategy for the construction of a full-length clone. The restriction map (*a*) was generated from nucleotide sequence analysis of clones VL16 (*b*) and VL18 (*c*). After digestion with *Eco*RI, the 5′ fragment of VL16 was ligated to the 3′ fragment of VL18 to form the full-length clone (*d*). The full-length clone was inserted into the expression vector (described in the text) via a 5′ *Hin*dIII linker and a 3′ *Bam*HI linker. The shaded portion of the restriction map (*a*) indicates the portion of the nucleotide sequence believed to code for the putative signal sequence. bp, Base pairs.

```
10 30 50 70 90
GAAACCGACACCACC ATG AAG ATA ATA ATT CTG TCT GTT ATA TTG GCC TAC TGT GTC ACC GAC AAC TGT CAA GAT GCA TGT CCT GTA GAA
Met Lys Ile Ile Ile Leu Ser Val Ile Leu Ala Tyr Cys Val Thr Asp Asn Cys Gln Asp Ala Cys Pro Val Glu
1 10 20

110 130 150 170
GCG GAA CCG CCA TCA AGT ACA CCA ACA GTT CCA ACT TCT TGT GAA GCT AAA GAA GGA GAA TGT ATA GAT ACC AGA TGC GCA ACA TGT AAA
Ala Glu Pro Pro Ser Ser Thr Pro Thr Val Pro Thr Ser Cys Glu Ala Lys Glu Gly Glu Cys Ile Asp Thr Arg Cys Ala Thr Cys Lys
30 40 50

190 210 230 250 270
CGA GAT ATA CTA TCA GAT GGA CTG TGT GAA AAT AAA CCA GGG AAG ACA TGC TGT AGA ATG TGC CAG TAT GTG ATT GAA TGC AGA GTA GAA
Arg Asp Ile Leu Ser Asp Gly Leu Cys Glu Asn Lys Pro Gly Lys Thr Cys Cys Arg Met Cys Gln Tyr Val Ile Glu Cys Arg Val Glu
60 70 80

290 310 330 350
GCA GCT GGT TAT TTT AGA ACG TTT TAC GGC AAA AGA TTT AAT TTT CAG GAA CCT GGT AAA TAT GTG CTG GCT AGG GGA ACC AAG GGT GGC
Ala Ala Gly Tyr Phe Arg Thr Phe Tyr Gly Lys Arg Phe Asn Phe Gln Glu Pro Gly Lys Tyr Val Leu Ala Arg Gly Thr Lys Gly Gly
90 100 110

370 390 410 430 450
GAT TGG TCT GTA ACC CTC ACC ATG GAG AAT CTA GAT GGA CAG AAG GGA GCT GTG CTG ACT AAG ACA ACA CTG GAG GTT GCA GGA GAC GTA
Asp Trp Ser Val Thr Leu Thr Met Glu Asn Leu Asp Gly Gln Lys Gly Ala Val Leu Thr Lys Thr Thr Leu Glu Val Ala Gly Asp Val
120 130 140

470 490 510 530
ATA GAC ATT ACT CAA GCT ACT GCA GAT CCT ATC ACA GTT AAC GGA GGA GCT GAC CCA GTT ATC GCT AAC CCG TTC ACA ATT GGT GAG GTG
Ile Asp Ile Thr Gln Ala Thr Ala Asp Pro Ile Thr Val Asn Gly Gly Ala Asp Pro Val Ile Ala Asn Pro Phe Thr Ile Gly Glu Val
150 160 170

550 570 590 610 630
ACC ATT GCT GTT GTT GAA ATA CCG GGC TTC [AAT ATC ACA] GTC ATC GAA TTC TTT AAA CTA ATC GTG ATT GAT ATT CTG GGA GGA AGA TCT
Thr Ile Ala Val Val Glu Ile Pro Gly Phe [Asn Ile Thr] Val Ile Glu Phe Phe Lys Leu Ile Val Ile Asp Ile Leu Gly Gly Arg Ser
180 190 200

650 670 690 710
GTG AGA ATT GCT CCA GAC ACA GCA AAC AAA GGA CTG ATA TCT GGT ATC TGT GGT AAT CTG GAG ATG AAT GAC GCT GAT GAC TTT ACT ACA
Val Arg Ile Ala Pro Asp Thr Ala Asn Lys Gly Leu Ile Ser Gly Ile Cys Gly Asn Leu Glu Met Asn Asp Ala Asp Asp Phe Thr Thr
210 220 230

730 750 770 790 810
GAT GCA GAT CAG CTG GCG ATC CAA CCC AAC ATA AAC AAA GAG TTC GAC GGC TGC CCA TTC TAT GGC AAT CCT TCT GAT ATC GAA TAC TGC
Asp Ala Asp Gln Leu Ala Ile Gln Pro Asn Ile Asn Lys Glu Phe Asp Gly Cys Pro Phe Tyr Gly Asn Pro Ser Asp Ile Glu Tyr Cys
240 250 260

830 850 870 890
AAA GGT CTG ATG GAG CCA TAC AGA GCT GTA TGT CGT AAC AAT ATC AAC TTC TAC TAT TAC ACT CTA TCC TGT GCC TTC GCT TAC TGT ATG
Lys Gly Leu Met Glu Pro Tyr Arg Ala Val Cys Arg Asn Asn Ile Asn Phe Tyr Tyr Tyr Thr Leu Ser Cys Ala Phe Ala Tyr Cys Met
270 280 290

910 930 950 970 990
GGA GGA GAA GAA AGA GCT AAA CAC GTC CTT TTC GAC TAT GTT GAG ACA TGC GCT GCG CCG GAA ACG AGA GGA ACG TGT GTT TTA TCA GGA
Gly Gly Glu Glu Arg Ala Lys His Val Leu Phe Asp Tyr Val Glu Thr Cys Ala Ala Pro Glu Thr Arg Gly Thr Cys Val Leu Ser Gly
300 310 320

1010 1030 1050 1070
CAT ACT TTC TAT GAC ACA TTC GAC AAA GCA AGA TAT CAA TTC CAG GGC CCA TGC AAG GAG ATT CTG ATG GCC GCA GAC TGT TAC TGG AAC
His Thr Phe Tyr Asp Thr Phe Asp Lys Ala Arg Tyr Gln Phe Gln Gly Pro Cys Lys Glu Ile Leu Met Ala Ala Asp Cys Tyr Trp Asn
330 340 350

1090 1110 1130 1150 1170
ACA TGG GAT GTA AAG GTT TCA CAT AGA GAC GTC GAA TCA TAC ACT GAG GTA GAG AAA GTA ACA ATC AGG AAA CAG TCA ACT GTA GTA GAT
Thr Trp Asp Val Lys Val Ser His Arg Asp Val Glu Ser Tyr Thr Glu Val Glu Lys Val Thr Ile Arg Lys Gln Ser Thr Val Val Asp
360 370 380

1190 1210 1230 1250
CTC ATT GTG GAT GGC AAG CAG GTC AAG GTT GGA GGA GTG GAT GTA TCT ATC CCG TAC AGC TCT GAG [AAC ACT TCC] ATA TAC TGG CAG GAT
Leu Ile Val Asp Gly Lys Gln Val Lys Val Gly Gly Val Asp Val Ser Ile Pro Tyr Ser Ser Glu [Asn Thr Ser] Ile Tyr Trp Gln Asp
390 400 410

1270 1290 1310 1330 1350
GGA GAC ATC CTG ACG ACG GCC ATC CTA CCT GAA GCT CTT GTC GTT AAG TTC AAC TTT AAG CAG CTC CTT GTA GTT CAT ATC AGA GAT CCA
Gly Asp Ile Leu Thr Thr Ala Ile Leu Pro Glu Ala Leu Val Val Lys Phe Asn Phe Lys Gln Leu Leu Val Val His Ile Arg Asp Pro
420 430 440

1370 1390 1410 1430
TTC GAT GGA AAG ACA TGC GGC ATA TGT GGT AAC TAT AAT CAA GAT TCA ACT GAT GAT TTC TTT GAC GCA GAA GGA GCA TGC GCT CTA ACC
Phe Asp Gly Lys Thr Cys Gly Ile Cys Gly Asn Tyr Asn Gln Asp Ser Thr Asp Asp Phe Phe Asp Ala Glu Gly Ala Cys Ala Leu Thr
450 460 470

1450 1470 1490 1510 1530
CCC AAC CCC CCA GGA TGT ACA GAG GAA CAG AAA CCA GAA GCT GAG CGA CTT TGC AAT AAT CTC TTT GAT TCT TCT ATC GAC GAG AAA TGT
Pro Asn Pro Pro Gly Cys Thr Glu Glu Gln Lys Pro Glu Ala Glu Arg Leu Cys Asn Asn Leu Phe Asp Ser Ser Ile Asp Glu Lys Cys
480 490 500

1550 1570 1590 1610
AAT GTC TGC TAC AAG CCT GAC CGG ATT GCC CGA TGT ATG TAC GAG TAT TGC CTG AGG GGA CAA CAA GGA TTT TGT GAC CAT GCT TGG GAG
Asn Val Cys Tyr Lys Pro Asp Arg Ile Ala Arg Cys Met Tyr Glu Tyr Cys Leu Arg Gly Gln Gln Gly Phe Cys Asp His Ala Trp Glu
510 520 530

1630 1650 1670 1690 1710
TTC AAG AAA GAA TGC TAC ATA AAA CAT GGA GAC ACT CTA GAA GTA CCA CCT GAA TGT CAA TAA ACGTACAAAGATACAGAAGCTAAGGCTACTACAGC
Phe Lys Lys Glu Cys Tyr Ile Lys His Gly Asp Thr Leu Glu Val Pro Pro Glu Cys Gln End
540 550

1730 1750 1770 1790 1810 1830
AGAAGATAAAAAAGAAACTGTAGTTCTTCAAAAACCGTGTATTTTATGTACTCATTGTTTAATTAGAGGAAAATAAATTGTTATTATCATAACTTAAAGTAAAAAAAAAAAAAAA
```

FIG. 3. Nucleotide sequence and predicted amino acid sequence of *Vargula* luciferase cDNA. Numbers above each line refer to nucleotide position and numbers below each line refer to amino acid position. Horizontal arrows indicate regions where the amino acid sequences were identical with those obtained by endopeptidase digestions. Consensus sequences for N-glycosylation are boxed, and the AATAAA polyadenylylation signal is underlined.

sequence overlap of 830 nucleotides. Nucleotide sequence analysis demonstrated that clone VL16 encodes the N-terminal portion of luciferase and clone VL18, the C-terminal portion. The complete nucleotide sequence of the *Vargula* luciferase cDNA is shown in Fig. 3 together with the deduced amino acid sequence.

The sequence contains an open reading frame of 1665 nucleotides coding for a protein of 555 amino acids with a calculated molecular weight of 62,171. The open reading frame contains the amino acid sequence used to construct the oligonucleotide probe. In addition, the amino acid sequences of seven other peptides determined by Edman degradation were in complete agreement with those deduced from the nucleotide sequence. The translation initiation codon was assigned to the first ATG codon at nucleotide position 16. The nucleotide sequence around the putative initiation codon is in

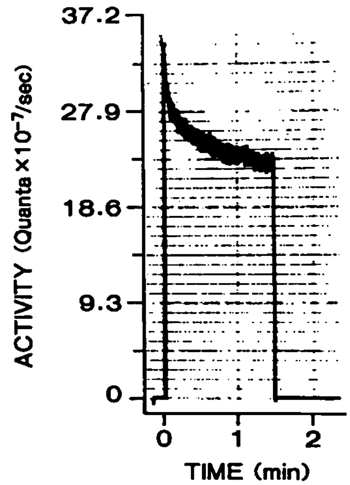

FIG. 4. Assay of active *Vargula* luciferase synthesized and secreted by COS cells. The cells, transfected with the expression plasmid pRSVVL, were incubated for 48 hr and the culture medium was assayed for luciferase activity in the presence of *Vargula* luciferin. Light emission was monitored with a Mitchell–Hastings (28) photometer attached to a Chromatocorder 12 (System Instruments). Shown above is the assay of the culture medium in which the transfected cells were incubated. A scintillation vial containing 100 μl of the culture medium was placed in the photometer and the shutter was opened. At time zero, 50 nM luciferin was injected into the vial and at 1.5 min the shutter was closed.

good agreement with the consensus sequence CC(A/G)CCAUGG, characteristic of many eukaryotic mRNAs (31). The N-terminal amino acid sequence also has many of the features of a signal sequence (32), in accord with the biological role of luciferase as a secretory protein.

Consistent with the positive staining of luciferase by the periodic acid–Schiff reaction, there are two potential N-glycosylation sites (Asn-Xaa-Ser/Thr), at amino acid residues 186 and 408. At residue 258 the sequence Asn-Pro-Ser occurs, but this sequence is generally not efficiently glycosylated (33). N-glycosidase F was found to reduce the molecular weight of luciferase by 2000–3000, while no reduction in molecular weight was detected in the digestions specific for O-glycosylation (data not shown). These results indicate that *Vargula* luciferase is N-glycosylated and that carbohydrate moieties may account for the difference in the calculated molecular weight of the polypeptide deduced from the nucleotide sequence and that measured for the native protein by gel electrophoresis (Fig. 1) and by gel filtration and sedimentation equilibrium analysis (34). The other notable feature of *Vargula* luciferase is the very cysteine-rich region present in the N-terminal portion, where nine cysteine residues can be found between amino acid residues 39 and 82.

Expression of *Vargula* Luciferase in COS Cells. To establish that the cloned cDNA actually encodes *Vargula* luciferase, a mammalian cell system was used to express the cDNA. As shown in Fig. 2, a full-length cDNA was constructed from clones VL16 and VL18, and it was placed under the promoter of the Rous sarcoma virus long terminal repeat. The hybrid gene was introduced into COS cells and the transfected cells were incubated for 48 hr. As shown in Fig. 4, luciferase activity was clearly detected in the culture medium of transfected COS cells with some luciferase activity also present in the cell extract. Luminescence from the media and cell extracts of COS cells which were either mock (no plasmid DNA) transfected or transfected with pSV0CAT (35) or pRSVL (24) was more than two orders of magnitude less intense than that shown in Fig. 4. These results confirm that the reconstructed cDNA is the full-length cDNA for *Vargula* luciferase and that it also encodes the signal for protein secretion. The luminescence emitted from the culture medium of COS cells was directly proportional to the volume of medium assayed, and a clear signal above background could be detected from as little as 5 μl of the 10 ml of culture medium obtained from COS cells transfected with the *Vargula* luciferase expression vector.

DISCUSSION

The present results are of interest not only because they contribute to a further understanding of the bioluminescent reaction in *Vargula* but also because they provide a more general understanding of the bioluminescent reactions of a large number of marine organisms in which structurally analogous luciferins and similar reaction mechanisms are used. Among these organisms, a direct comparison can now be made with the bioluminescent reaction of the jellyfish *Aequorea victoria* (36).

Aequorea possesses, in the margin of its umbrella, a calcium-binding protein, aequorin, which emits light in the presence of calcium ions. Aequorin is a complex of apoaequorin (apoprotein), coelenterazine, and molecular oxygen. When aequorin binds calcium ions, a conformational change takes place, converting the protein into an oxygenase. Coelenterazine is then oxidized via an intramolecular reaction, as shown in Fig. 5. The emitter in the reaction is the excited-state coelenteramide bound to apoaequorin (37). The cDNA for apoaequorin has been cloned and expressed, and subsequent analyses have shown apoaequorin to be composed of 189 amino acid residues (M_r = 21,400) with three EF-hand structures characteristic of Ca^{2+}-binding sites (9, 10, 38, 39).

Despite the close similarities in substrate structure and mechanisms of the bioluminescent reaction in *Vargula* and *Aequorea*, the enzymes and substrates of the two systems show only slight light-emitting cross-reactions. However, the two proteins are seen to show limited but significant amino acid sequence homologies in two regions of *Vargula* luciferase (residues 97–154 and 353–411) with one in apoae-

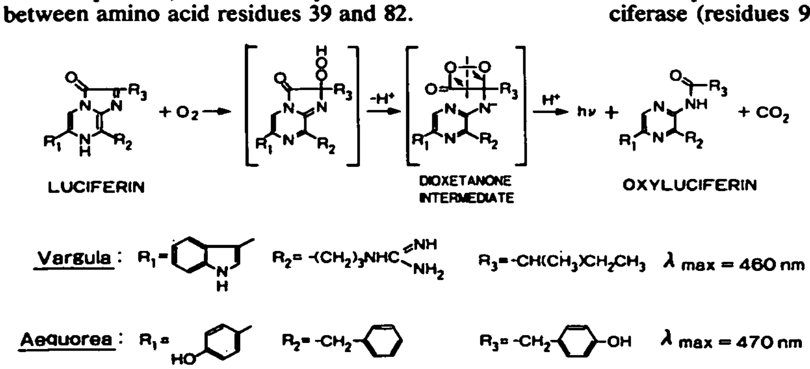

FIG. 5. Bioluminescence reactions of *Vargula* and *Aequorea*. In literature describing the *Aequorea* reaction, luciferin and oxyluciferin are also referred to as coelenterazine and coelenteramide, respectively.

```
    100                                     120                                     140
a   K R P N F Q E P G K Y V L A R G T K G G D W S V T L T H E N L D G Q K G A V L T K T T L E V A G D V I D I T Q A T A D
    : . . .   . :   . : : .   .     :         : .   . :   . .   . :   . . . . . . :   . .   .     . . .   . : . : . . . :
b   K K L A T D E L E K Y A K N E P T L I R I W G D A L - F D I V D K D Q N G A I T L D E W K A Y T K A A G I I Q S S E D
        90                                      110                                     130

                360                                     380                                     400
a   Y W N T W D V K V S H R D V E S Y T E V E K V T I R K Q S T V V D L I V D G K Q V K V G G V D V S I P Y S S E N T S I
    :   . . : .   : . .     . . : . : . .   :   .   : :     . . . .     : : :   . :     .   . . :       . : . . . . .   :
b   Y I E G W K - K L A T D E L E K Y A K N E P T L I R I W G D A L F D I V D K D Q N G A I T L D E W K A Y T K A A G I I
                    90                                      110                                     130
```

FIG. 6. Sequence homology between *Vargula* luciferase (*a*) and jellyfish (*Aequorea*) aequorin (*b*). Double dots indicate identical residues and single dots indicate amino acids with homologous scores in the Dayhoff mutation data matrix (40). Numbers indicate the position of each residue with respect to the N terminus of each protein.

quorin (residues 82–144) (Fig. 6). Since the entire apoaequorin molecule consists of 189 amino acid residues, about one third the number in *Vargula* luciferase, it is conceivable that one or both of the homologous regions in *Vargula* luciferase may be involved in light emission. The larger size of *Vargula* luciferase may also be due to its hydrolase activity (8). Possibly, it optimizes the luminescent reaction in seawater, in contrast to the aequorin reaction, which occurs intracellularly.

Since the N terminus of *Vargula* luciferase is blocked, it was not possible to determine which amino acid residue constitutes the N terminus of the mature polypeptide. However, considering the fact that the region in *Vargula* luciferase (residues 97–154) homologous to aequorin (residues 87–144) is shifted by 10 amino acid residues, it is possible that, as an approximation, the leader peptide for secretion is the first 11 amino acid residues and that the N terminus of luciferase is tyrosine (residue 12; Fig. 3). Should such a peptide be cleaved, it is likely to be at position 11, since alanine and the adjacent amino acid residues possess a pattern compatible with a signal sequence cleavage site (32).

Vargula luciferase does not appear to contain any clear EF-hand structures characteristic of calcium-binding sites, as present in aequorin. Consequently the previously reported inhibition of *Vargula* luciferase by EDTA (41) may be attributed to a different action from the inhibition observed with aequorin. Examination of the primary structure of *Vargula* luciferase reveals the presence of a relatively high content of glutamic and aspartic residues, as in aequorin. There is also a high content of cysteine residues. Since no free sulfhydryl group was detected in *Vargula* luciferase (34), the cysteine residues presumably exist in intramolecular disulfide bridges.

The *lux* operon of the bacterium *Vibrio fischeri* (42) and the luciferase gene of the firefly *Photinus pyralis* (24, 43) have been used as indicators of promoter activity and in other applications (44). The simplicity and specificity of the *Vargula* reaction, involving only the substrate luciferin and molecular oxygen, the high sensitivity with which light can be measured, and the fact that *Vargula* luciferase is secreted into the culture medium, suggest that the *Vargula* luciferase gene may find wide biomedical applications.

We thank Dr. Y. Haneda and Mr. M. Hayashi for assistance in the collection of *Vargula* and Dr. M. Nishizawa of Osaka Bioscience Institute for helpful discussions. This work was supported in part by research grants (DMB 85-17578 and DMB 88-44459) from the National Science Foundation (to F.I.T.), a Grant-in-Aid (62480131) from the Ministry of Education, Science and Culture of Japan (to S.N.), and a postdoctoral fellowship from the Science and Technology Agency of Japan (to E.M.T.).

1. Harvey, E. N. (1952) *Bioluminescence* (Academic, New York), pp. 297–331.
2. Kornicker, L. S. & Baker, J. H. (1977) *Proc. Biol. Soc. Wash.* **90**, 218–231.
3. Harvey, E. N. (1917) *Am J. Physiol.* **42**, 318–341.
4. Johnson, F. H. & Shimomura, O. (1978) *Methods Enzymol.* **57**, 331–364.
5. Kishi, Y., Goto, T., Hirata, Y., Shimomura, O. & Johnson, F. H. (1966) in *Bioluminescence in Progress*, eds. Johnson, F. H. & Haneda, Y. (Princeton Univ. Press, Princeton, NJ), pp. 89–113.
6. Stone, H. (1968) *Biochem. Biophys. Res. Commun.* **31**, 386–391.
7. Shimomura, O. & Johnson, F. H. (1971) *Biochem. Biophys. Res. Commun.* **44**, 340–346.
8. Shimomura, O., Johnson, F. H. & Masugi, T. (1969) *Science* **164**, 1299–1300.
9. Inouye, S., Noguchi, M., Sakaki, Y., Takagi, Y., Miyata, T., Iwanaga, S., Miyata, T. & Tsuji, F. I. (1985) *Proc. Natl. Acad. Sci. USA* **82**, 3154–3158.
10. Prasher, D., McCann, R. O. & Cormier, M. J. (1985) *Biochem. Biophys. Res. Commun.* **126**, 1259–1268.
11. Tsuji, F. I., Haneda, Y., Lynch, R. V., III, & Sugiyama, N. (1971) *Comp. Biochem. Physiol.* **40A**, 163–179.
12. Sie, E. H.-C., McElroy, W. D., Johnson, F. H. & Haneda, Y. (1961) *Arch. Biochem. Biophys.* **93**, 286–291.
13. Johnson, F. H., Sugiyama, N., Shimomura, O., Saiga, Y. & Haneda, Y. (1961) *Proc. Natl. Acad. Sci. USA* **47**, 486–489.
14. Thompson, E. M., Toya, Y., Nafpaktitis, B. G., Goto, T. & Tsuji, F. I. (1988) *J. Exp. Biol.* **137**, 39–51.
15. Tsuji, F. I. (1978) *Methods Enzymol.* **57**, 364–372.
16. Chirgwin, J. M., Przybyla, A. E., MacDonald, R. J. & Rutter, W. J. (1979) *Biochemistry* **18**, 5294–5299.
17. Aviv, H. & Leder, P. (1972) *Proc. Natl. Acad. Sci. USA* **69**, 1408–1412.
18. Morishita, K., Kubota, N., Asano, S., Kaziro, Y. & Nagata, S. (1987) *J. Biol. Chem.* **262**, 3844–3851.
19. Caruthers, M. H. (1987) in *Synthesis and Applications of DNA and RNA*, ed. Narang, S. A. (Academic, New York), pp. 47–94.
20. Benton, W. D. & Davis, R. W. (1977) *Science* **196**, 180–182.
21. Wahl, G. M., Stern, M. & Stark, G. R. (1979) *Proc. Natl. Acad. Sci. USA* **76**, 3683–3687.
22. Sanger, F., Nicklen, S. & Coulson, A. R. (1977) *Proc. Natl. Acad. Sci. USA* **74**, 5463–5467.
23. Chen, E. Y. & Seeburg, P. H. (1985) *DNA* **4**, 165–170.
24. deWet, J. R., Wood, K. V., DeLuca, M., Helinski, D. R. & Subramani, S. (1987) *Mol. Cell. Biol.* **7**, 725–737.
25. Gluzman, Y. (1981) *Cell* **23**, 175–182.
26. Graham, F. L. & van der Eb, A. J. (1973) *Virology* **52**, 456–467.
27. Wigler, M., Pellicer, A., Silverstein, S. & Axel, R. (1978) *Cell* **14**, 725–731.
28. Mitchell, G. W. & Hastings, J. W. (1971) *Anal. Biochem.* **39**, 243–250.
29. Hastings, J. W. & Weber, G. (1963) *J. Opt. Soc. Am.* **53**, 1410–1415.
30. Ohtsuka, E., Matsuki, S., Ikehara, M., Takahashi, Y. & Matsubara, K. (1985) *J. Biol. Chem.* **260**, 2605–2608.
31. Kozak, M. (1978) *Cell* **15**, 1109–1123.
32. von Heijne, G. (1983) *Eur. J. Biochem.* **133**, 17–21.
33. Marshall, R. D. (1972) *Annu. Rev. Biochem.* **41**, 673–702.
34. Tsuji, F. I., Lynch, R.V., III, & Stevens, C. L. (1974) *Biochemistry* **13**, 5204–5209.
35. Gorman, C. M., Moffat, L. F. & Howard, B. H. (1982) *Mol. Cell. Biol.* **2**, 1044–1051.
36. Johnson, F. H. & Shimomura, O. (1978) *Methods Enzymol.* **57**, 271–291.
37. Shimomura, O. & Johnson, F. H. (1973) *Tetrahedron Lett.*, 2963–2966.
38. Prasher, D. C., McCann, R. O., Longiaru, M. & Cormier, M. J. (1987) *Biochemistry* **26**, 1326–1332.
39. Kurose, K., Inouye, S., Sakaki, Y. & Tsuji, F. I. (1989) *Proc. Natl. Acad. Sci. USA* **86**, 80–84.
40. Dayhoff, M. O., Schwartz, R. M. & Orcutt, B. C. (1978) in *Atlas of Protein Sequence and Structure* (National Biomedical Research Foundation, Washington, DC), Vol. 5, pp. 345–352.
41. Lynch, R. V., III, Tsuji, F. I. & Donald, D. H. (1972) *Biochem. Biophys. Res. Commun.* **46**, 1544–1550.
42. Engebrecht, J., Simon, M. & Silverman, M. (1985) *Science* **227**, 1345–1347.
43. Ow, D. W., Wood, K. V., DeLuca, M., deWet, J. R., Helinski, D. R. & Howell, S. H. (1986) *Science* **234**, 856–859.
44. Hauber, R., Miska, W., Schleinkofer, L. & Geiger, R. (1988) *J. Clin. Chem. Clin. Biochem.* **26**, 147–148.

Proc. Natl. Acad. Sci. USA
Vol. 94, pp. 3402–3407, April 1997
Neurobiology

Patterns of synaptic activity in neural networks recorded by light emission from synaptolucins

(neurotransmission/exocytosis/optical imaging)

GERO MIESENBÖCK AND JAMES E. ROTHMAN

Cellular Biochemistry and Biophysics Program, Memorial Sloan–Kettering Cancer Center, 1275 York Avenue, New York, NY 10021

Contributed by James E. Rothman, December 30, 1996

ABSTRACT **The emission of light, coupled to exocytosis, can in principle be utilized to monitor the activity of a large number of individual synapses simultaneously. To illustrate this concept, fusion proteins of *Cypridina* luciferase and synaptotagmin-I or VAMP-2/synaptobrevin (which we term "synaptolucins") were expressed in cultured hippocampal neurons with the help of viral vectors. Synaptolucins were targeted to synaptic vesicles and, upon exocytosis, formed light-emitting complexes with their cognate luciferin, which was added to the extracellular medium. Photon emissions required a depolarizing stimulus, occurred from regions with high synaptic density as ascertained by vital staining of recycling synaptic vesicles, and were sensitive to Ca^{2+} depletion and clostridial neurotoxins. The method can currently detect exocytosis of the readily releasable pool of synaptic vesicles at a hippocampal synapse, corresponding to about two dozen quanta, but has the potential for greater sensitivity.**

Many problems in neurophysiology can be reduced to questions about the location, timing, and magnitude of synaptic activity, including, for instance, the integration of inputs by a single neuron, synaptic plasticity, and pattern classification and storage by neural networks. The study of these and related problems would greatly benefit from a method that allows direct recording from many synapses simultaneously, with the capacity to reliably detect single exocytotic events. Such a method would appear optimal because, on the one hand, central synapses generally transmit information via the fusion of a single synaptic vesicle (1, 2), while, on the other hand, the computational power of the nervous system arises from networks containing large numbers of synapses (3–5).

While current electrophysiological methods allow the activity of individual synapses to be recorded, they do not permit populations to be studied. There is a practical limit to the number of cells that can be impaled simultaneously with intracellular electrodes, and importantly, an invasive method requires an *a priori* decision on which cells to study, making discovery difficult. Extracellular field recordings with multiple electrodes avoid some of these problems and thereby allow the collective activities of many cells to be measured, but do not permit activity to be ascribed to individual synapses or neurons (6, 7). Optical imaging of light emission from fluorescent indicators of membrane potential or intracellular Ca^{2+} concentration (7–10) greatly increases spatial resolution but again, does not measure synaptic activity directly. An alternative optical approach that offers a direct gauge of synaptic activity is to load synaptic vesicles with fluorescent dyes and to observe dye release (11, 12). However, this method is intrinsically incapable of resolving individual quanta, which can cause only a small decrease in total fluorescence. Despite their limitations, these techniques have opened a window on multicellular phenomena as diverse as the representation of visual scenes by retinal ganglion cells (13) and the emergence of cortical circuits during development (14). Methods that reveal the detailed patterns of synaptic inputs and outputs in entire networks can thus be expected to disclose important new physiological concepts operative at the relatively unexplored interface between cellular and systems neurophysiology.

An ideal method for studying patterns of synaptic activity would consist of an optical signal that reports the act of transmitter release directly, allows detection of every vesicle fusion event, can be regenerated for many rounds of recording, and—less obvious from the above—originates from a genetically encoded probe (i.e., a protein). Genetic control would allow recordings to be obtained from cells, cultures, brain slices, or exposed tissues of transgenic animals, and would afford means to focus on individual neurons (by localized DNA transfer techniques), types of neurons (by cell-type specific promoters), or elements of a circuit (by recombinant viral vectors that spread through synaptic contacts; see ref. 15). We have designed a first generation of such probes, which we term "synaptolucins," and now report their construction and validation.

MATERIALS AND METHODS

Synaptolucins. Total *Cypridina* RNA extracted with Trisolv (Biotecx Laboratories, Houston) served as the template for the reverse transcriptase–PCR synthesis of a cDNA encoding the luciferase (16). The PCR product was subcloned into the amplicon plasmid pα4"a" (17, 18), and its sequence was determined with Sequenase 2.0 (United States Biochemical). To construct synaptolucins-1 and -2, the appropriate portions of the ORFs for *Cypridina* luciferase (16) and, respectively, synaptotagmin-I (19) and VAMP-2/synaptobrevin (20, 21) were fused via stretches of nucleotides encoding the flexible linker -(Ser-Gly-Gly)$_4$-.

The amplicon plasmids were transfected into E5 cells (17, 22) with the help of LipofectAMINE (GIBCO/BRL), and replicated and packaged into virions after infection with 0.1 pfu/cell of the herpes simplex virus (HSV) deletion mutant *d*120 (22). The primary virus stock was passaged on E5 cells until the vector-to-helper ratio exceeded 1:4; the ratio was estimated as the number of synaptolucin-positive Vero cells [by immunostaining, using mAbs M48 (23) and CL69.1 (24)] vs. the number of viral plaques formed after infection of E5 cells.

PC12 Cells. PC12 cells were infected at a multiplicity of 1 amplicon virion/cell and at 6 h *p.i.* harvested in buffer H (10 mM Hepes-NaOH, pH 7.4/150 mM NaCl/0.1 mM $MgCl_2$/1 mM EGTA/1 mM phenylmethylsulfonyl fluoride/1 μg/ml each of aprotinin, leupeptin, and pepstatin). Homogenates were prepared by 13 passes through a ball-bearing cell cracker

The publication costs of this article were defrayed in part by page charge payment. This article must therefore be hereby marked "*advertisement*" in accordance with 18 U.S.C. §1734 solely to indicate this fact.

0027-8424/97/943402-6$2.00/0
PNAS is available online at http://www.pnas.org.

Abbreviation: HSV, herpes simplex virus.

and postnuclear supernatants (5 min at 5000 × *g*) fractionated on 5–25% (wt/vol) glycerol gradients in a Beckman SW41 rotor, operated for 2 h at 41,000 rpm (25). Gradient fractions were analyzed by SDS/PAGE, Western blotting, and immunostaining.

To measure synaptolucin activities, postnuclear supernatants were solubilized on ice with 1% Nonidet P-40, clarified (10 min at 15,000 × *g*) and diluted 50-fold into buffer L (20 mM Hepes-NaOH, pH 7.4/150 mM NaCl/2 mM $CaCl_2$/2 mM $MgCl_2$) that had been prewarmed to 30°C. After addition of *Cypridina* luciferin to 5 μM, photon fluxes were integrated for 10 sec in an LKB 1250 luminometer calibrated with a [^{14}C]hexadecane standard (26). Synaptolucin concentrations were determined by quantitative immunoblotting with mAbs M48 (23) and CL69.1 (24) and [^{125}I]protein G (New England Nuclear), using the recombinant cytoplasmic domains of synaptotagmin and VAMP as the standards.

Hippocampal Neurons. The hippocampal CA1–CA3 fields of P1 Sprague–Dawley rats were dissected into Earle's balanced salt solution with 10 mM Hepes-NaOH (pH 7.0) and mechanically dissociated after treatment with 20 units/ml papain (Worthington) (27, 28). Cells were plated onto the poly-D-lysine- and laminin-coated surface of 35-mm dishes with central 8-mm glass windows (adhesive substrates were from Sigma). The cultures were maintained in basal medium Eagle with Earle's salts and 25 mM Hepes-NaOH (pH 7.4), supplemented with 20 mM glucose, 1 mM sodium pyruvate, 10% fetal bovine serum, 0.1% Mito+ Serum Extender (Collaborative Biomedical Products, Bedford, MA), 100 units/ml penicillin, 0.1 mg/ml streptomycin, and from day 5 after plating, 5 μM cytosine arabinoside (Sigma) (28). The preparations were infected with HSV amplicon vectors after 1–2 weeks *in vitro*. Viral inocula were diluted to multiplicities of roughly 0.1 in conditioned medium containing 1 mM kynurenate (Fluka), adsorbed for 1 h, removed, and replaced with conditioned medium.

Optical Recording. At 8–20 h *p.i.*, culture dishes were transferred to a PDMI-2 microincubator (Medical Systems, Greenvale, NY) mounted on the stage of a Zeiss Axiovert 135 TV microscope and held at 30°C. A Teflon insert forming an 8-mm-wide channel across the optical window was placed in the dish to allow rapid perfusion with either normokalemic solution (25 mM Hepes-NaOH, pH 7.05/119 mM NaCl/2.5 mM KCl/2 mM $CaCl_2$/2 mM $MgCl_2$, 30 mM glucose) or its hyperkalemic counterpart (KCl raised to 90 mM, NaCl reduced to 31.5 mM). Nerve terminals were stained by a 1-min exposure to 3 μM FM 4-64 (Molecular Probes) in hyperkalemic solution (12) with 1% dialyzed bovine serum, followed by superfusion with normokalemic solution for >10 min.

FM 4-64 fluorescence was excited with the 510- to 560-nm band of an attenuated xenon arc lamp; alternatively, synaptolucin bioluminescence was initiated by adding 30 nM luciferin from a 30 μM methanolic stock. Emitted light was collected with a Zeiss ×40/1.3 NA Plan-Neofluar oil immersion objective, 590-nm longpass-filtered in the case of FM 4-64 fluorescence, and focused onto the photocathode of a C2400-30H image intensifier coupled to a C2400-75 charge-coupled device (both from Hamamatsu Photonics, Hamamatsu, Japan). The video signal was 8-bit digitized in an Argus-20 image processor (Hamamatsu Photonics) and saved to a Power Macintosh for analysis, using NIH IMAGE 1.60 (http://rsb.info.nih.gov/nih-image/), TRANSFORM 3.3 (Fortner Research LLC, Sterling, VA), and MATHEMATICA 3.0 (Wolfram Research, Champaign, IL).

RESULTS AND DISCUSSION

Synaptolucins. Synaptolucins are engineered membrane proteins consisting of two modules: a targeting module derived from a synaptic vesicle-specific integral membrane protein, such as synaptotagmin-I (19) or VAMP-2/synaptobrevin (20, 21), and a light-generating module that is constitutively "off" but is switched "on" in the instant of exocytosis. This translates transmitter release into an optical signal. In synaptolucins, the role of the switchable light-generating module is played by a luciferase, attached to the inner surface of synaptic vesicles and acting on a membrane-impermeant substrate. If the substrate is present in the extracellular medium and the enzyme sequestered in synaptic vesicles, light emission cannot occur, but once the vesicle fuses with the presynaptic membrane and the catalytic module is externalized, a burst of photon emission follows. For this strategy to be viable, the luciferase must (*i*) catalyze a sufficiently high photon flux for imaging (a quantity dependent on the enzyme's turnover number and the quantum yield of the light-emitting complex), (*ii*) use a membrane-impermeant substrate, (*iii*) be capable of folding in the endoplasmic reticulum lumen and be targetted to synaptic vesicles, and (*iv*) operate efficiently under the pH and salt conditions of the extracellular environment.

Of the well-characterized bioluminescent systems, that of the ostracod *Cypridina* (or *Vargula*) *hilgendorfii* (29) matches this profile remarkably well, in contrast to the commonly used firefly luciferase, which does not. *Cypridina* luciferase is a monomeric, naturally secreted glycoprotein of 62 kDa (16, 30) that can be expressed in and is secreted from transfected mammalian cells (31); firefly luciferase is peroxisomal. *Cypridina* luciferin (32) carries a guanidino group expected to be positively charged at physiological pH and to thereby render the molecule slowly permeant or even impermeant to membranes. Unlike firefly luciferase, which requires ATP (and, for sustained activity, coenzyme A), *Cypridina* luciferase uses no cofactors other than water and O_2 (29). Its luminescent reaction proceeds optimally at pH 7.2 and physiological salt concentrations (30), whereas that of firefly is optimal at low ionic strength (activity is inhibited 5- to 10-fold by physiological salt), alkaline pH, and reducing conditions. With a turnover number of 1600 min^{-1} (33) and a quantum yield of 0.29 (34), *Cypridina* luciferase produces a specific photon flux exceeding that of the optimized firefly system (35) by a factor of at least 50.

We isolated a cDNA encoding *Cypridina* luciferase and constructed two synaptolucins. In synaptolucin-1, the C terminus of luciferase is fused to the N terminus of synaptotagmin-I, located in the lumen of synaptic vesicles. The hybrid protein relies on the cleavable signal peptide encoded by the luciferase gene for membrane translocation and is anchored by the transmembrane domain of synaptotagmin. In synaptolucin-2, the mature N terminus of luciferase is fused to the C terminus of VAMP-2, located in the vesicle lumen. This results in a type II hybrid protein with a membrane-anchor segment that also serves as a noncleavable signal sequence. The luciferase cDNA we obtained (GenBank accession no. U89490) differed from the published DNA sequence (16) at 30 positions, only three of which gave rise to amino acid substitutions: Asp-16 → Val, Ile-346 → Leu, and Asn-495 → Ser. The first substitution shifted the predicted signal peptide cleavage site (16), leading us to consider Gln-19 the mature N terminus and to construct synaptolucin-2 accordingly.

When expressed in PC12 cells, the synaptolucin genes directed the synthesis of membrane proteins of the expected sizes which cosedimented with their respective targeting modules in velocity gradients (Fig. 1). The synaptolucins, like VAMP and synaptotagmin, were found both in synaptic vesicles (fractions 4–9) and endosomes (fractions 11–14) (25). Both synaptolucins were enzymatically active, with a k_{cat} of 5.2 and 3.7 photon emissions sec^{-1} per synaptolucin-1 and -2 molecule, respectively, determined as described in *Materials and Methods*.

Imaging Neurotransmitter Release. Initial experiments on hippocampal neurons, performed at a saturating luciferin

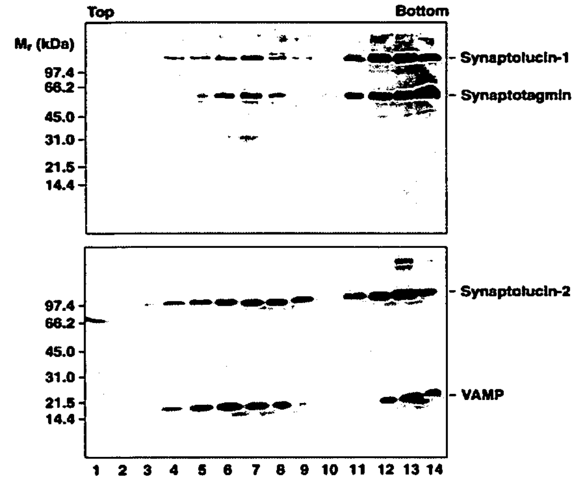

FIG. 1. Cofractionation of synaptolucins with synaptic vesicle proteins. Amplicon-infected PC12 cells were homogenized and post-nuclear supernatants sedimented into 5–25% glycerol gradients. Small synaptic vesicles band in fractions 4–9, endosomes in fractions 11–14 (25). The bottom fraction contains material collected on a sucrose cushion; compared with the slower-sedimenting fractions, only 15% of this material was analyzed by SDS/PAGE. Proteins were precipitated with trichloroacetic acid, separated on 8–18% gels, and transferred to nitrocellulose. The filters were probed with mAb M48 (23), directed against synaptotagmin-I (*Top*), or mAb CL69.1 (24), directed against VAMP-2 (*Bottom*). Bound antibodies were visualized by ECL (Amersham).

concentration of 5 μM (30), revealed an unexpected problem: a depolarizing stimulus was not required for photon emissions to occur. We suspected that this signal arose from the intracellular synaptolucin pool, which would become visible if *Cypridina* luciferin, an imidazo[1,2-a]pyrazine nucleus with mostly hydrophobic substitutions (32), crossed biological membranes once its guanidino group was deprotonated. We thus lowered the pH of our bath solutions from 7.4 to 7.05 to favor the protonated luciferin species, and decreased their luciferin content to reduce diffusion across membranes. Indeed, at a luciferin concentration of 30 nM, the background signal disappeared and photon emissions became stimulation-dependent. However, longer photon-counting times were required because at a luciferin concentration so far below the K_m of luciferase (0.52 μM; ref. 30), synaptolucin operated at only 3% of its V_{max}.

Fig. 2 illustrates a typical imaging experiment on hippocampal neurons infected with an HSV amplicon vector transducing synaptolucin-1. We first obtained a map of the synapses within the field of view (Fig. 2*A*) by taking the preparation through a depolarization cycle (12) in the presence of FM 4-64 (36), a member of the family of fluorescent dyes that are known to stain recycling synaptic vesicles (11). FM 4-64 was chosen over the more widely used FM 1-43 (11, 12) because it does not absorb significantly at 462 nm, the emission wavelength of *Cypridina* luciferin (34), and thus permits the acquisition of an unperturbed synaptolucin signal from a stained preparation. After perfusion with normokalemic solution for at least 10 min, sufficient to replenish the synaptic vesicle pool and to remove excess FM 4-64, we added a bolus of luciferin to the bath solution and counted photon emissions for the next 30 sec. In many cases, such as the one shown in Fig. 2*B*, some photons were registered in the absence of a depolarizing stimulus, but these originated mainly from regions without an appreciable density of synapses (compare the areas marked by dashed red lines in Fig. 2*A* and *B*). It is likely that HSV-infected glial cells in the mixed culture are the source of this background signal,

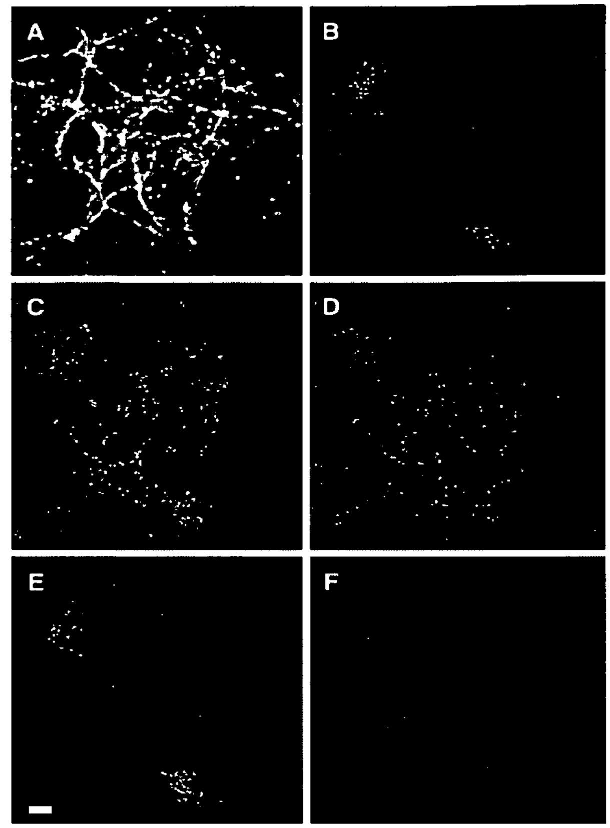

FIG. 2. Hippocampal neurons expressing synaptolucin-1, imaged by wide-field microscopy. About 60% of the neurons were infected by HSV transducing synaptolucin-1. (*A*) The synaptic map, revealed by loading nerve terminals with FM 4-64. The fluorescent signal from FM 4-64 was acquired at low intensifier gain and averaged over 32 video frames. (*B–E*) Photon registrations accumulated from synaptolucin emissions over 30 sec, obtained at 30 nM luciferin, maximum image intensifier gain, and a discriminator value for photon detection that suppressed background and equipment noise (photon counts in the presence of a depolarizing stimulus but the absence of luciferin) to an average of 1.06 photon registrations per 100-pixel field. The preparation was imaged successively in normokalemic solution (*B*) and during three hyperkalemic challenges to induce exocytosis, performed in either the presence (*C* and *D*) or the absence (*E*) of external Ca^{2+}. Ten minutes under resting conditions elapsed between each of the successive stimuli. The dashed red lines in *A–C* mark areas of stimulation-independent synaptolucin activity, in all likelihood due to virus-infected glial cells. (*F*) Superimposition of the synaptolucin signal of *C*, colored here in red, onto a binary version of the synaptic map. The binary map was constructed by thresholding *A* such that pixels with an intensity above the 97th percentile appear in black. (Bar = 20 μm.)

because the neurotropism of HSV in hippocampal cultures is incomplete (17), and because synaptotagmin, the targeting module of synaptolucin-1, appears at the cell surface when expressed in nonneuronal cells (37). This problem could be circumvented by using neuron-specific promoters.

To record light emission resulting from synaptic activation, the preparation was perfused with hyperkalemic solution to depolarize the neurons, open voltage-gated Ca^{2+} channels in presynaptic terminals, and trigger exocytosis. Because *Cypridina* luciferin is unstable in aqueous solution, decomposing with a $t_{1/2}$ on the order of 1 min (29, 30), a second bolus of luciferin was added immediately after depolarization, and photons were counted for 30 sec thereafter. A far greater number of photons were registered than in the absence of a

stimulus, and now their pattern (Fig. 2*C*) was similar to the synaptic map recorded with FM 4-64 (Fig. 2*A*). The match, however, was imperfect, presumably because the synaptolucin image contained background emissions from virus-infected glial cells (compare the areas marked by dashed red lines in Fig. 2 *B* and *C*), and because only a subset of synapses (those formed by neurons that are virus-infected) are potential light sources. Repeating the depolarization after a 10-min resting period evoked a similar but not entirely identical response (Fig. 2*D*), whereas depolarization without Ca^{2+} influx (by omitting free Ca^{2+} from the hyperkalemic solution) left the photon count at baseline level, with photon emissions only from the regions attributed to glial cells (compare Fig. 2 *E* and *B*).

To examine the degree of correspondence between the sites of synaptolucin activity and the synaptic map more rigorously, we overlaid, as depicted schematically in Fig. 2*F*, photon-counting images with a binary filter constructed from the synaptic map (Fig. 2*A*). The filter was chosen such that it "transmitted" only at pixels where the intensity of FM 4-64 fluorescence exceeded the 97th percentile of the grayscale (black areas in Fig. 2*F*) but blocked transmission elsewhere (gray areas in Fig. 2*F*). If such a digital filter scans another image and the intensity of the transmitted signal is plotted as a function of the relative shift between filter and image, maxima occur where the filter detects a matching structure in the image (38). Fig. 3 shows the result of scanning two synaptolucin images, Fig. 2 *B* and *C*, with a filter constructed from Fig. 2*A*. Clearly, the signal in Fig. 2*B* has no counterpart in the synaptic map, supporting its identification as a contaminant of nonneuronal origin (Fig. 3 *Lower*). The sites of evoked photon emissions in Fig. 2*C*, by contrast, produce a sharp maximum where filter and image are in register and thus map to nerve terminals (Fig. 3 *Upper*).

In addition to characteristic sensitivities to membrane potential and extracellular Ca^{2+}, an optical signal generated by synaptic vesicle exocytosis should be susceptible to clostridial neurotoxins that inactivate components of the machinery for transmitter release (39). Fig. 4 shows an experiment performed to address this point. An FM 4-64/synaptolucin image pair was first acquired to locate synaptolucin-expressing synapses (Fig. 4*A*). Following a second round of FM 4-64 loading (to compensate for dye release during acquisition of the synaptolucin image, see Fig. 4*B*), the preparation was incubated on the microscope stage with 20 nM each of botulinum neurotoxin serotypes B and F (39) plus 1 μM tetrodotoxin to suppress action potentials (and hence, dye release) during the incubation. After 3 h of toxin treatment a second pair of images was recorded, and noted to differ from the first in two respects: (*i*) the dimming of FM 4-64 fluorescence that originally accompanied the hyperkalemic challenge now failed to occur, indicating that exocytosis was effectively blocked (compare Fig. 4 *B* and *D*), and (*ii*) photon emissions from synaptolucin disappeared concomitantly (compare Fig. 4 *A* and *C*). This ties the synaptolucin signal firmly to the process of neurotransmitter release.

Potential Applications and Current Limitations. The reproducible pattern of photon registrations in repeated trials (compare Fig. 2 *C* and *D*) attests to the reliability of synaptolucins as indicators of exocytosis, with many possible applications. For example, the interpretation of many studies on synaptic plasticity is fraught with controversy, possibly because the pre- and postsynaptic components of neurotransmission cannot be distinguished by traditional methods, which are all indirect (40). Measuring exocytosis directly via synaptolucins, before and after maneuvers that alter synaptic strength, could help to resolve ambiguities. Or, the multiple inputs to a postsynaptic neuron could be mapped with the help of synaptolucins. If the postsynaptic neuron's membrane potential is monitored electrically, the shape of a synaptic potential as it arrives after propagation through the dendritic tree could be measured and immediately correlated with its anatomical site

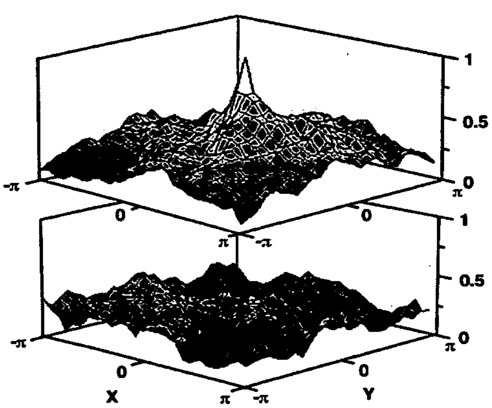

FIG. 3. Matched filtering of two synaptolucin images, Fig. 2 *B* (control) and *C* (exocytosis triggered), with their common synaptic map, Fig. 2*A*, as shown schematically in Fig. 2*F*. The *x*- and *y*-axes indicate the relative shifts between filter and image in these projections, and the ordinate the normalized cross-correlation function, a measure of the match between image and filter (38). The function is computed by pointwise multiplication in the spatial frequency domain and, due to the properties of the Fourier transform, periodic (38). Only a single period, from $-\pi$ to π in the *x*- and *y*-directions, is shown. At shift (0,0), filter and image are in register, at shifts $(x, \pm\pi)$ or $(\pm\pi, y)$, the filter's center is displaced to an edge of the image. (*Upper*) Scanning of Fig. 2*C*, showing evoked synaptolucin emissions. Note the peak at a filter shift of (0,0), indicating a matching structure in the image. (*Lower*) Scanning of Fig. 2*B*, lacking evoked synaptolucin emissions. Note the absence of a central peak.

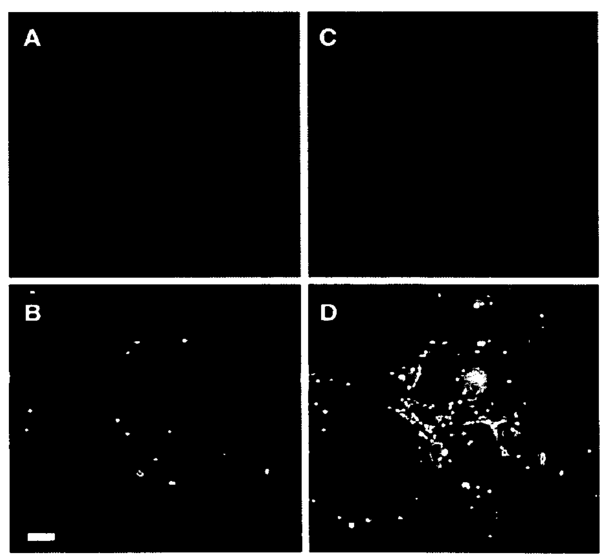

FIG. 4. Hippocampal neurons expressing synaptolucin-1, imaged by wide-field microscopy at the same intensifier and detector settings as in Fig. 2. (*Upper*) Photon registrations from synaptolucin emissions during the first 30 sec after triggering exocytosis, colored in red and superimposed on synaptic maps obtained with FM 4-64. (*Lower*) FM 4-64 images after a 30-sec hyperkalemic challenge. *A* and *B* were recorded before and *C* and *D* after treatment with botulinum neurotoxins B and F. Botulinum neurotoxins were applied during a 5-min depolarization (to enhance toxin uptake into recycling synaptic vesicles) and then during a 3-h incubation in complete medium with 1 μM tetrodotoxin. Note the marked decrease in FM 4-64 fluorescence intensity in *B* as opposed to *D*. (Bar = 20 μm.)

Table 1. Vesicle fusion events at single synapses

Method of estimation	No. of fusion events	Photons emitted per vesicle	Photon emission rate per vesicle, sec^{-1}
Kinetics of transmitter release	67	4.7	0.38
Photon count fluctuations	51	6.1	0.49

Synaptic vesicle exocytosis and recycling were modeled as Poisson processes (1, 2, 41, 42), using kinetic parameters obtained in studies of transmitter or dye release from identified synapses of hippocampal neurons in culture (12, 43, 44). This stochastic model provided the basis for estimating the number of fusion events, either on the assumption of a fixed number of statistically independent release sites per synapse (41–43), or through an analysis of photon count fluctuations (45, 46), using the data displayed in Table 2. (The mathematical details are available by e-mail from g-miesenboeck@ski.mskcc.org.)

of origin, with important implications for input integration (5). The pattern of activation of individual synaptic inputs could be measured in relation to the activation of a postsynaptic neuron, affording a direct means of establishing firing rules.

Does current synaptolucin technology allow for these applications, each of which would require the ability to detect light emitted from the fusion of a single synaptic vesicle? The sensitivity and temporal resolution afforded by synaptolucins are determined by three factors: the number of synaptolucin molecules per vesicle, their specific emission rate, and the time over which photon counts can be integrated to keep pace with the relevant physiology. At video rates, this interval is usually a single video frame, or about 30 msec. At the other extreme, with long photon-counting times as in the present experiments, the timing of the synaptic vesicle cycle itself becomes limiting. In such cases, photon emission begins as a vesicle fuses with the presynaptic membrane, probabilistically (41, 42) at any time during the observation period, and ends as its synaptolucins are re-internalized, again probabilistically, or the camera shutter is closed. Vesicle recycling will terminate synaptolucin activity virtually instantaneously: if luciferin is taken up by recycling vesicles at its bulk concentration of 30 nM, only about 1 in a 1000 recycled vesicles will contain a luciferin molecule (as can be calculated from the internal diameter of a synaptic vesicle of 50 nm), and those few that do will consume the internalized luciferin (via luciferase) rapidly. This effectively prevents the visualization of endocytosed vesicles and limits photon emissions to the synaptolucin's dwell time in the presynaptic membrane.

Estimates for the number of quanta released under our experimental conditions and for the average observation time per synaptolucin can be derived by modelling vesicle release and recycling as Poisson processes (1, 2, 41, 42). At a typical hippocampal synapse, the probability for exocytosis drops from an initial rate of about 20 quanta sec^{-1} (the "readily releasable pool") to a basal rate of 2 quanta sec^{-1} (43); the transition between initial and basal release rates occurs exponentially with a time constant of 1.2 sec (43). The probability of recycling is assumed constant throughout, with a $t_{1/2}$ of 20 sec (12, 44). When such a synapse is observed for 30 sec under maintained hyperkalemic stimulation, an average of 67 quantal releases will take place (Table 1), and the synaptolucins contained in one quantum (i.e., one vesicle) will emit for an average of 13 sec (see the legend to Table 1). Under the same conditions, an average of 12 photon registrations were counted per synapse (Table 2). Correcting for the detection efficiency (see Table 2), this translates into about 310 photon emissions for the entire synapse, 4.7 photon emissions for a single vesicle, and a photon emission rate of 0.38 sec^{-1} per vesicle (Table 1), equalling that generated by about three synaptolucin molecules *in vitro* at the same limiting luciferin concentration of 30 nM.

A fluctuation analysis (45, 46) of the photon counts in Table 2, obtained from the experiment shown in Fig. 2*C*, estimates the number of released quanta as 51 per synapse and the photon emission rate as 0.49 sec^{-1} per vesicle, in rather close agreement with the values derived from kinetic arguments alone (Table 1).

Comparing the number of photon registrations (about 12 per synapse) with the actual number of vesicle fusion events (about 60 per synapse) indicates that the majority of fusion events remained undetected with present technology. With a photon emission rate of 0.4–0.5 sec^{-1} per vesicle (Table 1) and an overall photon detection efficiency of about 4% (Table 2), the time between two successive photon registrations from synaptolucins originating in the same vesicle (the waiting time for the stochastic process) would average about 50 sec. This is considerably longer than the average 13 sec for which a synaptolucin was observed. Hence under our present conditions, synaptolucins will often be re-internalized before a single photon emission can be detected, and those vesicle fusion events that do register cannot be precisely located on a temporal scale.

Future Prospects. Initial experiments with synaptolucins have established the feasibility of a potentially important new principle for functional analysis of neural networks—the coupling of light emission to synaptic vesicle exocytosis to provide a direct optical image of synaptic activity. However, while it has been shown that synaptolucins can faithfully record the averaged properties of many vesicle fusion events, the present sensitivity is too low for the detection of single exocytotic events.

Improvements that should allow synaptolucins to perform at the level of single quanta, with increased reliability and better temporal resolution, can be readily envisaged. First, we now must employ luciferin at subsaturating concentrations to minimize its penetration into cells, limiting luciferase to about 3% of its maximum velocity. Use of a truly membrane impermeant luciferin derivative at saturating concentrations would increase photon emissions about 35-fold. Second, there are currently only about three light-generating modules per synaptic vesicle in the HSV-infected neurons. This number could be increased (*i*) by gene replacement technology to fully substitute synaptolucins for VAMP and/or synaptotagmin and (*ii*) by including multiple light-generating modules in a single synaptolucin. Singly,

Table 2. Photon counts

Photon counts per field	Efficiency			Photons emitted per field
	Collection	Detection	Overall	
12 ± 3.9	0.29	0.13	0.04	310

The gray-level increment corresponding to a single photon count was determined from the histogram of Fig. 2*C*, and the number of photon registrations over a 30-sec period counted in fifty 2 × 2-pixel fields, corresponding to 1.8 × 1.8-μm areas in the specimen plane. These fields were selected by two criteria: (*i*) FM 4-64 fluorescence in excess of the 97th percentile (see Fig. 2*F*), and (*ii*) a >5-fold increase in synaptolucin activity upon depolarization. To convert photon counts to photon emissions, two correction factors were used: the collection efficiency of a 1.3 NA oil immersion objective, defined as the fraction of photons emitted from the focal plane that fall into the objective's acceptance cone, and the detection efficiency of the intensifier photocathode (C2400-30H; Hamamatsu Photonics) at 462 nm.

or in combination, these engineering steps should permit reliable detection of single vesicle fusion events at every visible synapse.

We are greatly indebted to Dr. Osamu Shimomura for his generosity in providing *Cypridina* luciferin. We also thank Dr. Yoshiaki Toya for the *Cypridina*, Dr. Dora Ho for pα4"a", Dr. Neal DeLuca for E5 cells and HSV strain *d*120, Dr. Giampietro Schiavo for botulinum neurotoxins, and Dr. Qais Al-Awqati for his thoughtful comments on the manuscript. This work was supported by the Mathers Charitable Foundation and by postdoctoral fellowships from the Austrian Fonds zur Förderung der wissenschaftlichen Forschung and the Charles H. Revson and Charles A. Dana Foundations.

1. Redman, S. (1990) *Physiol. Rev.* **70,** 165–198.
2. Stevens, C. F. & Wang, Y. (1995) *Neuron* **14,** 795–802.
3. Anderson, J. A. & Rosenfeld, E., eds. (1988) *Neurocomputing* (MIT Press, Cambridge, MA).
4. Shepherd, G. M., ed. (1990) *The Synaptic Organization of the Brain* (Oxford Univ. Press, Oxford), 3rd Ed.
5. McKenna, T., Davis, J. & Zornetzer, S. E., eds. (1992) *Single Neuron Computation* (Academic, Boston).
6. Meister, M., Pine, J. & Baylor D. A. (1994) *J. Neurosci. Methods* **51,** 95–106.
7. Stenger, D. A. & McKenna, T. M., eds. (1994) *Enabling Technologies for Cultured Neural Networks* (Academic, San Diego).
8. Grinvald, A. (1985) *Annu. Rev. Neurosci.* **8,** 263–305.
9. Tsien, R. Y. (1989) *Annu. Rev. Neurosci.* **12,** 227–253.
10. Tsien, R. Y. & Waggoner, A. (1995) in *Handbook of Biological Confocal Microscopy*, ed. Pawley, J. B. (Plenum, New York), 2nd Ed., pp. 267–279.
11. Betz, W. J. & Bewick, G. S. (1992) *Science* **255,** 200–203.
12. Ryan, T. A., Reuter, H., Wendland, B., Schweizer, F., Tsien, R. W. & Smith, S. J. (1993) *Neuron* **11,** 713–724.
13. Meister, M. (1996) *Proc. Natl. Acad. Sci. USA* **93,** 609–614.
14. Katz, L. C. & Shatz, C. J. (1996) *Science* **274,** 1133–1138.
15. Kuypers, H. G. J. M. & Ugolini, G. (1990) *Trends Neurosci.* **13,** 71–75.
16. Thompson, E. M., Nagata, S. & Tsuji, F. I. (1989) *Proc. Natl. Acad. Sci. USA* **86,** 6567–6571.
17. Ho, D. Y. (1994) *Methods Cell Biol.* **43,** 191–210.
18. Lawrence, M. S., Ho, D. Y., Dash, R. & Sapolsky, R. M. (1995) *Proc. Natl. Acad. Sci. USA* **92,** 7247–7251.
19. Perin, M. S., Fried, V. A., Mignery, G. A., Jahn, R. & Südhof, T. C. (1990) *Nature (London)* **345,** 260–263.
20. Elferink, L. A., Trimble, W. S. & Scheller, R. H. (1989) *J. Biol. Chem.* **264,** 11061–11064.
21. Südhof, T. C., Baumert, M., Perin, M. S. & Jahn, R. (1989) *Neuron* **2,** 1475–1481.
22. DeLuca, N. A., McCarthy, A. M. & Schaffer, P. A. (1984) *J. Virol.* **56,** 558–570.
23. Matthew, W. D., Tsavaler, L. & Reichardt, L. F. (1981) *J. Cell Biol.* **91,** 257–269.
24. Edelmann, L., Hanson, P. I., Chapman, E. R. & Jahn, R. (1995) *EMBO J.* **14,** 224–231.
25. Clift-O'Grady, L., Linstedt, A. D., Lowe, A. W., Grote, E. & Kelly, R. B. (1990) *J. Cell Biol.* **110,** 1693–1703.
26. Hastings, J. W. & Weber, G. (1963) *J. Opt. Soc. Am.* **53,** 1410–1415.
27. Huettner, W. J. & Baughman, R. W. (1986) *J. Neurosci.* **6,** 3044–3060.
28. Geppert, M., Goda, Y., Hammer, R. E., Li, C., Rosahl, T. W., Stevens, C. F. & Südhof, T. C. (1994) *Cell* **79,** 717–727.
29. Johnson, F. H. & Shimomura, O. (1978) *Methods Enzymol.* **57,** 331–364.
30. Shimomura, O., Johnson, F. H. & Saiga, Y. (1961) *J. Cell. Comp. Physiol.* **58,** 113–124.
31. Inouye, S., Ohmiya, Y., Toya, Y. & Tsuji, F. J. (1992) *Proc. Natl. Acad. Sci. USA* **89,** 9584–9587.
32. Kishi, Y., Goto, T., Hirata, Y., Shimomura, O. & Johnson, F. H. (1966) *Tetrahedron Lett.* **29,** 3427–3436.
33. Shimomura, O., Johnson, F. H. & Masugi, T. (1969) *Science* **164,** 1299–1300.
34. Shimomura, O. & Johnson, F. H. (1970) *Photochem. Photobiol.* **12,** 291–295.
35. Wulff, K. (1981) in *Bioluminescence and Chemiluminescence*, eds. DeLuca, M. A. & McElroy, W. D. (Academic, New York), p. 219.
36. Henkel, A. W. & Betz, W. J. (1995) *J. Neurosci.* **15,** 8246–8258.
37. Feany, M. B., Yee, A. G., Delvy M. L. & Buckley, K. M. (1993) *J. Cell Biol.* **123,** 575–584.
38. Duda, R. O. & Hart, P. E. (1973) *Pattern Classification and Scene Analysis* (Wiley, New York).
39. Montecucco, C. & Schiavo, G. (1995) *Q. Rev. Biophys.* **28,** 423–472.
40. Bliss, T. V. P. & Collingridge, G. L. (1993) *Nature (London)* **361,** 31–39.
41. Katz, B. (1969) *The Release of Neural Transmitter Substances* (Liverpool Univ. Press, Liverpool, U.K.).
42. Bekkers, J. M. & Stevens, C. F. (1995) *J. Neurophysiol.* **73,** 1145–1156.
43. Stevens, C. F. & Tsujimoto, T. (1995) *Proc. Natl. Acad. Sci. USA* **92,** 846–849.
44. Ryan, T. A., Smith, S. J. & Reuter, H. (1996) *Proc. Natl. Acad. Sci. USA* **93,** 5567–5571.
45. Katz, B. & Miledi, R. (1972) *J. Physiol. (London)* **224,** 665–699.
46. Neher, E. & Stevens, C. F. (1977) *Annu. Rev. Biophys. Bioeng.* **6,** 345–381.